Title
Design of a versatile chemical assembly method for patterning colloidal nanoparticles

Journal
Nanotechnology, 20(6)

ISSN
0957-4484

Authors
Choi, JH
Adams, SM
Ragan, R

Publication Date
2009-02-11

DOI
10.1088/0957-4484/20/6/065301

Nanotechnology **20** (2009) 065301 (6pp) doi:10.1088/0957-4484/20/6/065301

Design of a versatile chemical assembly method for patterning colloidal nanoparticles

J H Choi, S M Adams and R Ragan

Chemical Engineering and Materials Science, University of California Irvine, Irvine, CA 92697, USA

E-mail: rragan@uci.edu

Received 24 October 2008, in final form 20 November 2008
Published 14 January 2009
Online at stacks.iop.org/Nano/20/065301

Abstract

Poly(methyl methacrylate) (PMMA) domains in phase-separated polystyrene-*b*-poly(methyl methacrylate) (PS-*b*-PMMA) diblock copolymer thin films were chemically modified for controlled placement of solution synthesized Au nanoparticles having a mean diameter of 24 nm. Colloidal Au nanoparticles functionalized with thioctic acid were immobilized on amine functionalized PMMA domains on the PS-*b*-PMMA template using 1-ethyl-3-[3-dimethylaminopropyl] carbodiimide hydrochloride linking chemistry and *N*-hydroxy sulfosuccinimide stabilizer. Atomic force microscopy and scanning electron microscopy images demonstrated immobilization of Au nanoparticles commensurate with PMMA domains. Nanoparticles form into clusters of single particles, dimers, and linear chains as directed by the PMMA domain size and shape. Capillary forces influence the spacing between Au nanoparticles on PMMA domains. Inter-particle spacings below 3 nm were achieved and these assemblies of closely spaced nanoparticle clusters are expected to exhibit strong localized electromagnetic fields. Thus, these processes and material systems provide an experimental platform for studying resonantly enhanced excitations of surface plasmons as a function of material and geometric structure as well as utilization in catalytic applications.

(Some figures in this article are in colour only in the electronic version)

1. Introduction

The unique optical [1], electrical [2], and chemical [3] properties of nanoparticles have generated considerable interest since metal nanoparticle based architectures have shown the capacity for single molecule detection via the strong near-field coupling between closely spaced nanoparticles in sensors [4] and utility as two-dimensional photonic devices [5]. In addition, metallic nanoparticles supported on substrates have been demonstrated to have increased catalytic performance as compared to their bulk counterparts [6]. While lithographic top-down methods have advantages over bottom-up methods for producing ordered arrays, enhanced optical [7] and catalytic [6] properties have been observed when inter-particle spacing and minimum feature size, respectively, are in the sub-10 nm regime. Bottom-up methods are able to produce nanostructures in this regime; yet for many applications, device fabrication requires control of size, shape, as well as placement of metal nanoparticles on surfaces that is not always achievable via self-assembly.

Self-organization of metal colloids does offer the ability for control of size [8], shape [9], and interfaces [10] of sub-10 nm metal nanoparticles since solution-phase nanoparticle synthesis offers control of these parameters at nanometer length scales. Metal colloids assembled on patterned templates then allow for control of nanoparticle placement. Lithographic templates have previously been defined where gravitational effects or capillary forces dominate assembly [11, 12]. Lithography has also been combined with layer-by-layer assembly [13] or self-assembled monolayers [14] in which electrostatic interactions and/or capillary forces predominantly drive assembly. Using near-field lithography, the minimum particle size and periodicity reported by the above techniques is 50 nm and slightly greater than 0.5 μm, respectively [12]. Here

we report the use of diblock copolymers as a self-organized chemical template rather than lithographically defined physical templates for assembling metal nanoparticles from colloids. Au nanoparticles have been assembled on domains as small as 20 nm and in the case of single particles on chemical domains a periodicity of 46 nm was achieved; this constitutes an important step toward scaling down architectures achieved via metal colloid assembly on templates.

In this work, spherical Au nanoparticles having a mean diameter of 24 nm were assembled onto chemically modified poly(methyl methacrylate) (PMMA) domains on polystyrene-*b*-poly(methyl methacrylate) (PS-*b*-PMMA) diblock copolymer surfaces. In the case of hexagonally closed packed PMMA domains in a PS matrix the periodicity was measured as 46 ± 2.7 nm (1σ). Solution synthesis of Au nanoparticles in a stable colloid was performed since this offers a higher degree of control of size, material, and shape than physical vapor deposition of Au at these nanometer length scales. Self-organized PS-*b*-PMMA diblock copolymer thin films are attractive as a template [15] since the size and patterns of PMMA domains in PS-*b*-PMMA templates can be controlled using molecular weight [16] and processing conditions [17]. Furthermore, advances in diblock copolymer processing have demonstrated the ability to fabricate self-organized polymer surfaces with hexagonal arrangement [18], lamellae [19], and even lamellae with 45°–135° turns [20] having negligible defect density. Thus, the fabrication method of Au nanoparticle array assembly described here can be generalized to fabricate diverse array architectures with a variety of materials having controllable geometry on the nanoscale.

2. Experimental details

The schematic of figure 1 illustrates the three key steps of the chemical assembly process for selective placement of Au nanoparticles on self-organized PS-*b*-PMMA templates in which (a) size and shape controlled Au nanoparticles with thioctic acid ligands in a colloidal solution are exposed to (b) chemically modified PMMA domains on PS-*b*-PMMA diblock copolymer templates and (c) 1-ethyl-3-[3-dimethylaminopropyl] carbodiimide hydrochloride (EDC) linking chemistry with *N*-hydroxy sulfosuccinimide (S-NHS) [21] is utilized to form a covalent bond between Au nanoparticles and the PMMA domains for selective immobilization of thioctic acid functionalized Au nanoparticles on PMMA domains versus the PS matrix. Au nanoparticles on PS-*b*-PMMA templates were characterized using an Ultra 55 scanning electron microscopy (Carl Zeiss, Germany) and a MFP 3D scanning probe microscope (Asylum Research, Santa Barbara, USA).

Synthesis of sodium citrate stabilized Au nanoparticle colloids with a particle size of 24 ± 4 nm (1σ) as measured by SEM was performed in solution using the Turkevich method [22]. Chemical functionalization of colloidal Au nanoparticles with thioctic acid was accomplished by the addition of 1 ml of 0.1 mM DL-6,8-thioctic acid (Sigma-Aldrich) dissolved in ethanol to 100 ml of Au colloid having a pre-adjusted pH of 11 in order to avoid nanoparticle

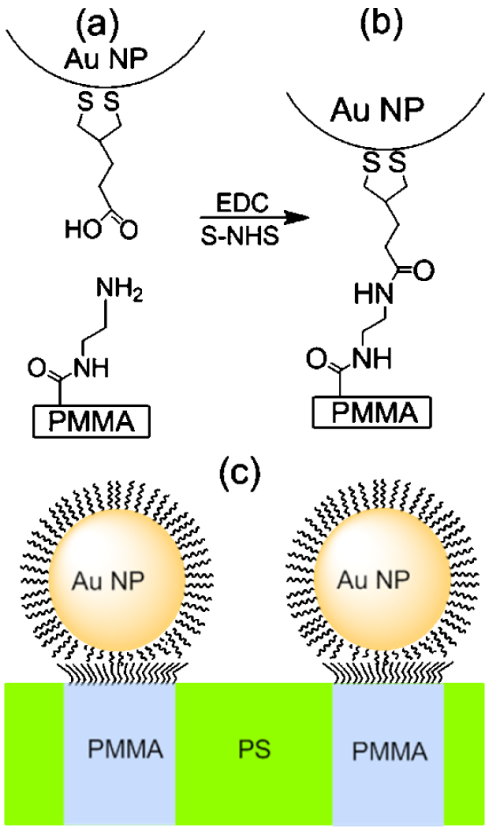

Figure 1. Schematic representation of assembly method: (a) Au nanoparticles are functionalized with thioctic acid and the PS-*b*-PMMA diblock copolymer template has been chemically modified to functionalize PMMA domains with amine groups; (b) cross-linking Au nanoparticles with –COOH functional groups and PMMA with $–NH_2$ functional groups using EDC and S-NHS chemistry; (c) TA-Au nanoparticles assembled on PMMA domains on PS-*b*-PMMA template.

aggregation. The solution was then stirred for 18 h. Thioctic acid functionalized Au (TA-Au) nanoparticles in colloidal solution were centrifuged for 15 min (at 11 000G, 22 °C), followed by decantation of supernatants and subsequent dispersal into Millipore Milli-Q de-ionized water.

PS-*b*-PMMA template fabrication was performed on Si substrates after cleaning the Si substrate by removing the native oxide layer with an aqueous solution of 10 vol% hydrofluoric acid (49%) for 2 min and then rinsing with de-ionized water. Before PS-*b*-PMMA was deposited, a random copolymer (Polymer Source, Inc. Dorval, Canada) having number average molar mass (Mn) and weight average molar mass (Mw) of 7.4 kg mol^{-1} and 11.8 kg mol^{-1}, respectively, was deposited. The solution has 1 wt% PS-r-PMMA in a toluene solvent and was spin coated at 3000 rpm for 40 s and then annealed at 168 °C for 72 h under vacuum to allow the end groups with α-hydroxy-ω-tempo moiety to diffuse and react with the Si surface and anchor PS-r-PMMA to Si substrate [23]. PS-r-PMMA not attached was removed with toluene leaving an approximate 5–6 nm film of anchored PS-r-PMMA as measured by ellipsometry. After, a 1 wt% PS-*b*-PMMA in toluene solution was spin coated at 3000 rpm onto the Si substrate for 60 s. The films were then annealed at 168 °C

Table 1. Contact wetting angles of water on PS-*b*-PMMA, PMMA, and PS surfaces measured before and after submersion in ethylenediamine solution.

Polymer surface	PS-*b*-PMMA	PMMA	PMMA sheet (from [26])	PS	PS (from [27])
Contact angle (before exposure to ethylenediamine)	85° ± 1°	68° ± 3°	76° ± 4°	85° ± 1°	86° ± 2°
Contact angle (after exposure to ethylenediamine)	70° ± 3°	58° ± 5°	57° ± 5°	84° ± 1°	—

(well above the T_g of 105 °C) in vacuum to facilitate microphase separation of the two polymer domains and provide polymer mobility. The PS-*b*-PMMA template was sonicated in isopropanol and de-ionized water (50:50) for 5 min and then dried completely by high purity Ar gas.

3. Results and discussion

Typical PS-*b*-PMMA templates that were obtained using a diblock copolymer having Mn of 170 kg mol^{-1} (PS) and 14.5 kg mol^{-1} (PMMA) and following the described fabrication method above are shown in the 1 μm × 1 μm AFM (a) topography (b) and phase images of figure 2. The AFM images were obtained in AC mode with a repulsive tip-sample interaction. The topography image in figure 2(a) shows only slight contrast due to the different phases and a height undulation across the surface. In contrast, PMMA and PS regions are clearly distinguishable in the phase images of figure 2(b). PMMA appears darker than PS under repulsive imaging conditions [24] due to the fact that PMMA has a higher modulus than PS at room temperature [24]. In order to modify PMMA surface chemistry on the PS-*b*-PMMA templates, the samples were submerged into 1.5 vol% solution of ethylenediamine in dimethyl sulfoxide for 5 min and then rinsed with isopropanol stream. The AFM images of figures 2(c) and (d) show topography and phase, respectively, of the PS-*b*-PMMA templates after surface treatment. Line profiles (shown in figure 2(e)) of the PS-*b*-PMMA surface before (solid line) and after (open circles) immersion in the ethylenediamine solution were taken from the sections indicated by a white line in figures 2(a) and (c), respectively. These line profiles demonstrate that PMMA preferentially reacts with the ethylenediamine solution in that PMMA regions are selectively etched. An etched depth of approximately 3–4 nm for PMMA domains on PS-*b*-PMMA templates after ethylenediamine exposure is observed as compared with the relatively flat surface before exposure.

Contact angle wetting at ambient temperature using a Model 100-07 contact angle goniometer (Rame-Hart, Inc.) was measured to further investigate changes in surface chemistry on PS-*b*-PMMA templates due to ethylenediamine exposure. Contact angles of pure PS and pure PMMA thin films were also measured in order to compare with observed changes in PS-*b*-PMMA templates; contact angle values are listed in table 1. The contact angle of a PS-*b*-PMMA template was measured as 85° ± 1° (1σ) and 70° ± 3° (1σ) before and after ethylenediamine surface treatment, respectively (table 1, col. 2). Thus, the surface becomes more hydrophilic after 5 min of ethylenediamine exposure. Similarly, pure PMMA surfaces become more hydrophilic after surface treatment; the contact angle of a pure PMMA thin films before and after immersion in the ethylenediamine solution for 5 min was measured as 68° ± 3° (1σ) and 58° ± 5° (1σ), respectively (table 1, col. 3). This is consistent with the formation of amine groups on PMMA since primary amine groups on PMMA are more hydrophilic than ester groups on an untreated PMMA surface as reported previously (table 1, col. 4) [26]. In order to investigate the reactivity of the PS surface regions on the PS-*b*-PMMA template, the measured contact angles of pure PS thin film were measured as approximately 85° ± 1° (1σ) for the untreated PS surface (table 1, col. 5) and is consistent with values reported in the literature (table 1, col. 6) [27]. The contact angle was measured as approximately 84° ± 1° (1σ) for the PS surface exposed to the ethylenediamine solution for 15 min (table 1, col. 5). From these results it can be inferred

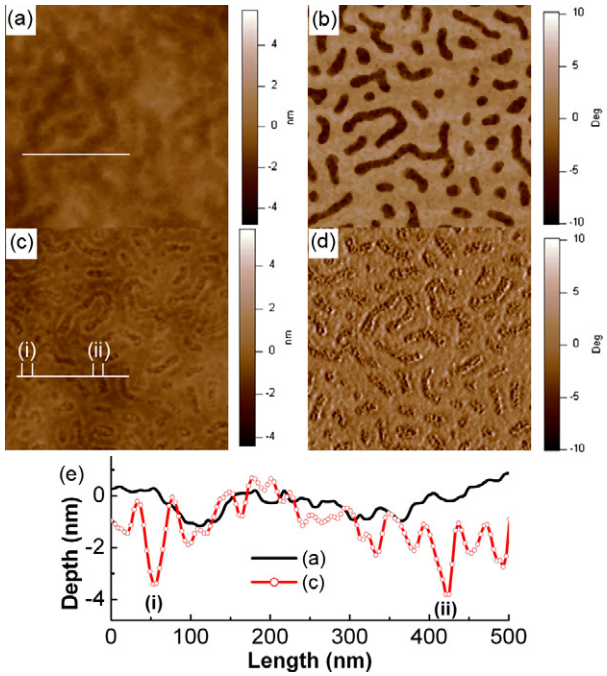

Figure 2. 1 μm × 1 μm AFM images of PS-*b*-PMMA diblock copolymer template showing (a) topography and (b) phase contrast as prepared and (c) topography and (d) phase contrast after surface treatment with ethylenediamine. (e) Line profiles as prepared (solid black line) and after exposure to ethylenediamine (red open circle-line) of the sections highlighted by a white line on (a) and (c), respectively.

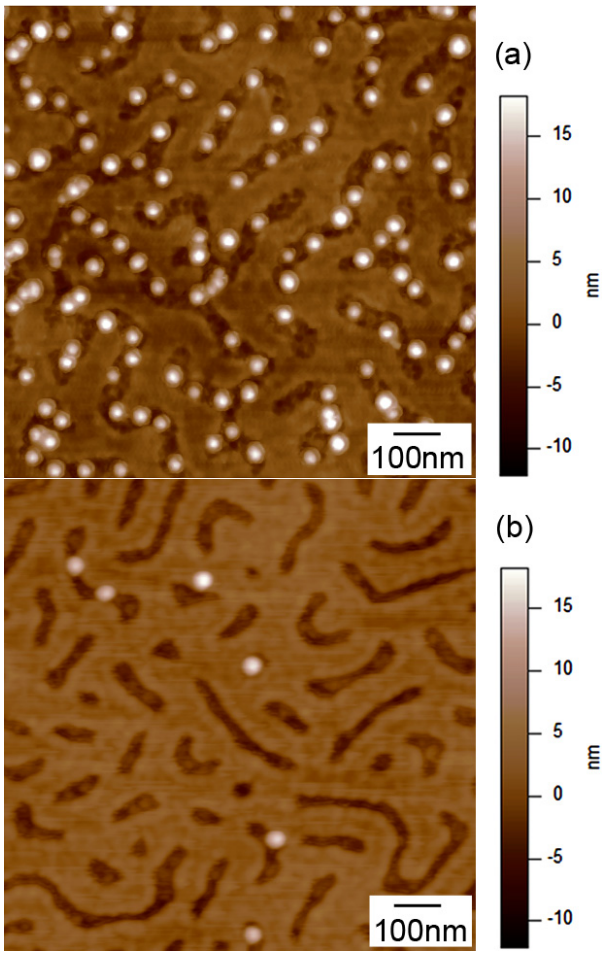

Figure 3. 1 μm × 1 μm AFM topography images acquired after incubation of TA-Au nanoparticles (Au nanoparticle concentration $\approx 18.6 \times 10^{11}$ ml^{-1}) on PS-*b*-PMMA templates exposed to ethylenediamine (a) with EDC and S-NHS and (b) without EDC and S-NHS incorporated in the process.

that PS does not react significantly with ethylenediamine since the contact angle of PS film remains nearly unchanged. Since the areal density of PMMA domains on PS-*b*-PMMA template was calculated as approximately 26% from the phase contrast image in figure 2(b), it is expected that the change in contact angle on the PS-*b*-PMMA template would not be as large as that observed on the pure PMMA thin film. Thus, the change in the contact angle observed in the PS-*b*-PMMA template after exposure to the ethylenediamine solution is indicative of chemical modification of PMMA domains.

After surface treatment, PS-*b*-PMMA templates were then immersed into the TA-Au colloidal solution having a pH of 5.5 and then incubated at 45 °C for 2 h. At the same time, 10 μl of an EDC solution (2 mM) and 10 μl of an S-NHS solution (5 mM) that were both dissolved in 2-(*N*-morpholino)ethanesulfonic acid were added to 1 ml of TA-Au colloid to promote interaction between COOH functional groups on Au nanoparticles and NH_2 functional groups on PMMA domains. This reaction is expected to lead to covalent cross-linking between the TA-Au nanoparticles and chemically modified PMMA domains since EDC forms an amine-reactive O-acylisourea and S-NHS converts amine-reactive O-acylisourea to amine-reactive S-NHS ester [21]. The samples were then rinsed with isopropanol and completely dried with high purity Ar gas. In order to evaluate the importance of EDC/S-NHS coupling chemistry on Au nanoparticle immobilization, TA-Au colloids having fixed Au nanoparticle concentration of approximately 18.6×10^{11} ml^{-1} were exposed to PS-*b*-PMMA templates under two different incubation conditions, with and without EDC and S-NHS. After exposure to TA-Au colloids, the templates were rinsed with isopropanol while spinning at 2000 rpm on a spin coater. AFM topography images of templates exposed to TA-Au colloids with EDC and S-NHS and without EDC and S-NHS are shown in figures 3(a) and (b), respectively. Au nanoparticles are distributed on dark PMMA domains when EDC and S-NHS was incorporated in the process (figure 3(a)). Alternatively, only a few Au nanoparticles adhered on PS-*b*-PMMA templates without EDC and S-NHS (figure 3(b)). Au nanoparticle adhesion on PMMA domains likely results from electrostatic interactions as observed in other systems [13, 28].

The relationship between PMMA domain size and shape and the nanoparticle cluster arrangement was investigated and

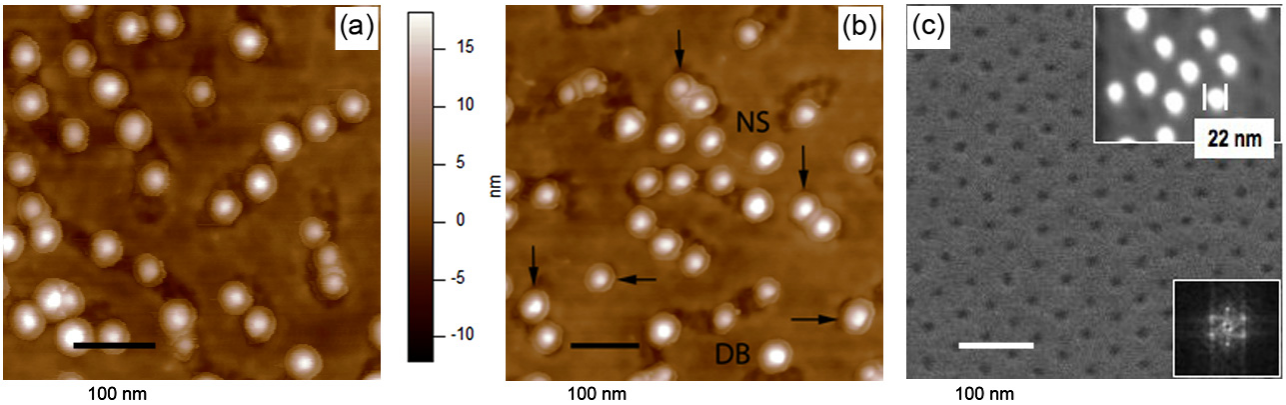

Figure 4. (a) and (b) 500 nm × 500 nm AFM height images of TA-Au nanoparticles immobilized on chemically modified lamellar PMMA domains. In (b), horizontal arrows indicate isolated nanoparticles and vertical arrows indicate dimers. Particles attached to domain boundaries 'DB' and non-specific interactions 'NS' are also designated. (c) SEM image of PS-*b*-PMMA template having hexagonally close packed PMMA cylinders oriented normal to the surface. The inset shows TA-Au nanoparticles that adopt the hexagonal pattern of template. The FFT spectrum of the image in (c) is also shown as an inset and was used to calculate the center-to-center spacing of the PMMA domains.

structures are shown in the AFM topography and SEM images of figure 4. Although the nanoparticles coverage on PMMA domains is not 100%, if one examines domains that have high nanoparticle coverage in the 500 nm × 500 nm AFM image of figure 4(a) it is clear that TA-Au nanoparticles follow the curved path of the PMMA domains and form chains of nanoparticles. Smaller PMMA domains sizes are observed in the 500 nm × 500 nm AFM image of figure 4(b). Isolated nanoparticles are observed when the PMMA domain size is on the order of the TA-Au nanoparticle diameter (vertical arrows) and dimers are formed for slightly larger domains (horizontal arrows). These results are consistent with prior observations of micron [29] and sub-micron [12] sized polymer (PS) beads assembled on lithographically fabricated templates with a cluster size that is determined by the patterned domain size.

Yet when the domain size and nanoparticle diameter are similar, it is not completely clear if nanoparticles are on a PMMA domain or are on PS. In order to confirm the placement of TA-Au nanoparticle on small PMMA domains, the PS-*b*-PMMA fabrication process was modified slightly by using a different diblock copolymer precursor having Mn of 55 kg mol^{-1} (PS) and 22 kg mol^{-1} (PMMA). From this process hexagonally close packed PMMA domains are obtained on the surface of the PS-*b*-PMMA template. Figure 4(c) shows a SEM image of such a PS-*b*-PMMA template. The PMMA regions appear darker than PS regions on the templates due to etching that occurs during exposure to the ethylenediamine solution. The inset in figure 4(c) shows that when the nanoparticle diameter is approximately equal to the PMMA domain size only one nanoparticle is immobilized on the PMMA domain and the hexagonal pattern of the template is adopted by the nanoparticles. Thus control of domain size and nanoparticle coverage can produce tunable arrays of nanoparticles on polymer templates.

From figure 4(b), it is observed that some nanoparticles attach to domain boundaries rather than the center of the domain and are labeled with 'DB'. Other nanoparticles appear to have non-specific interactions with the surface and are labeled 'NS' in figure 4(b). Templates were exposed to TA-Au colloids with varying nanoparticle concentrations to investigate the probability of specific/non-specific interactions occurring between nanoparticles and template. The PS-*b*-PMMA templates shown in the SEM images figure 5 were exposed to the ethylenediamine solution for 15 min and thereby the observed height contrast allows one to determine the number of TA-Au nanoparticles that adhere to PMMA versus PS on the template. It was observed that by increasing Au nanoparticle concentration in colloids ((a) ≈4.65 × 10^{11} particles ml^{-1}, (b) ≈9.3 × 10^{11} particles ml^{-1}, (c) ≈13.9 × 10^{11} particles ml^{-1}, (d) ≈18.6 × 10^{11} particles ml^{-1}), the coverage of Au nanoparticles on PMMA domains was determined to increase from 14% to 44%. A larger population of multiparticle clusters such as dimers, trimers, and linear chains results with increased coverage but does not result in uncontrolled aggregation that was observed in previous work using diblock copolymers as templates without modification of copolymer surface chemistry [30]. Summarized in figure 5(e) is the

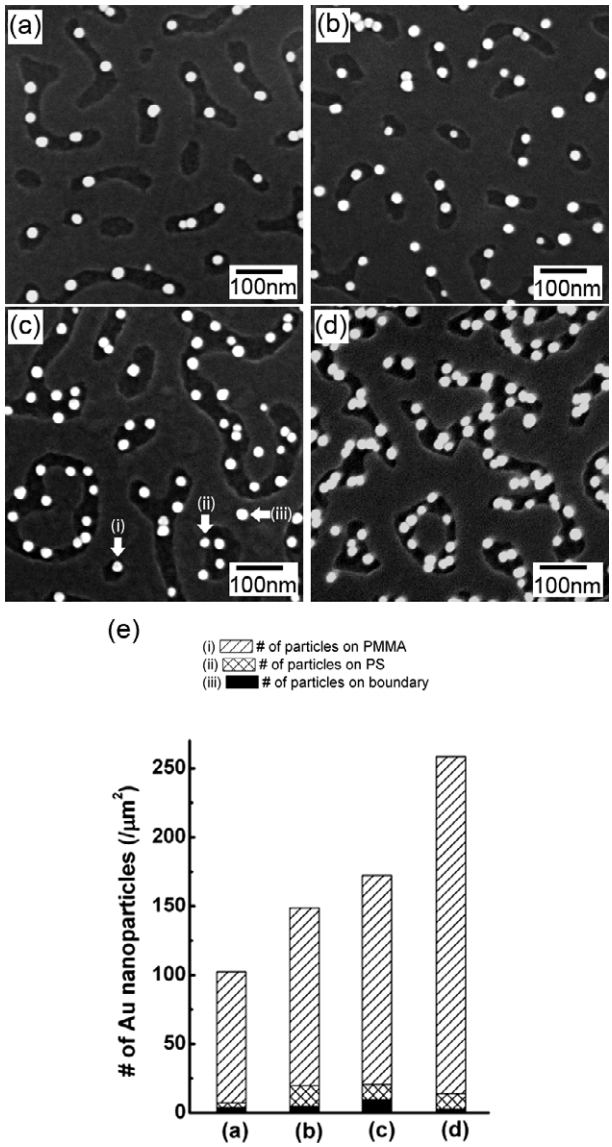

Figure 5. SEM images of TA-Au nanoparticles on chemically modified PS-*b*-PMMA templates after incubation with Au colloids having various TA-Au nanoparticle concentration: (a) ≈4.65 × 10^{11} ml^{-1}, (b) ≈9.3 × 10^{11} ml^{-1}, (c) ≈13.9 × 10^{11} ml^{-1} and (d) ≈18.6 × 10^{11} ml^{-1}. The nanoparticles labeled with (i), (ii), and (iii) show what represents a nanoparticle attached to PMMA, PMMA-PS domain boundary and PS, respectively. The normalized number of particles per square micron on PMMA domains (diagonal hatching), attached to PS-PMMA domain boundaries (solid black) and on PS (cross hatching) as a function of TA-Au nanoparticle concentration in colloidal solution as determined from the SEM images of (a)–(d).

normalized number of particles per square micron on PMMA domains, labeled with (i), attached to PS-PMMA domain boundaries, labeled with (ii), and on PS, labeled with (iii), as a function of nanoparticle concentration in the colloid obtained from SEM images having an approximate area of one square micron (with the exception of the column labeled with (a) that had an area of 5.4 × 10^5 nm^2). As coverage increases, there is a sharp increase in the number of nanoparticles attached to PMMA domains. The number of TA-Au nanoparticles

found on domain boundaries and non-specifically bound to PS remains relatively constant and thereby appears to be a random process that is dependent on surface area rather than nanoparticle concentration in the colloid. It has been found previously that non-specific interactions can be minimized by engineering a repulsive surface charge on the template matrix material [12, 29] and will be employed in future work.

4. Conclusions

In summary, SEM and AFM images demonstrate that colloidal TA-Au nanoparticles were preferentially immobilized on chemically modified PMMA domains on PS-*b*-PMMA diblock copolymer templates using EDC and S-NHS linking chemistry. Thus, self-organized templates and covalent substrate-nanoparticle interactions have been used to overcome limitations to pattern nanoparticles with nanometer scale periodicity on the order of 40 nm and avoid uncontrolled aggregation. By producing a variety of chemical domain sizes, we show that single particles, dimers, nanochain, etc can be assembled into clusters on surfaces with nanometer scale inter-particle spacing. Diblock copolymer templates have demonstrated versatility in array architectures that can be generated. Solution-phase metal nanoparticle synthesis allows for control of size, shape, interfaces, and material. Thereby the combination of diblock copolymer templates and metal colloids has great potential for patterning diverse assemblies of noble metal nanoparticles for fundamental studies of plasmonic coupling, fabrication of two-dimensional photonic devices, and for catalytic applications.

Acknowledgments

The authors wish to thank C Strohhoefer (Fraunhofer IZM) and V Jankovic (NGC) for input during scientific discussions. This work was supported by UC Discovery Pilot Projects for multidisciplinary research program with Northrop Grumman Corporation as the corporate sponsor and the National Science Foundation CBET-0642217.

References

[1] Mie G 1908 *Ann. Phys. (Berlin)* **25** 377
Gans R 1912 *Ann. Phys. (Berlin)* **37** 881
[2] Collier C P, Saykally R J, Shiang J J, Henrichs S E and Heath J R 1997 *Science* **277** 1978
[3] Haruta M, Tsubota S, Kobayashi T, Kageyama H, Genet M J and Delmon B 1993 *J. Catal.* **144** 175
[4] Nie S and Emory S R 1997 *Science* **275** 1102
Kneipp K, Wang Y, Kneipp H, Perelman L T, Itzkan I, Dasari R and Feld M S 1997 *Phys. Rev. Lett.* **78** 1667
[5] Brongersma M L, Hartman J W and Artwater H A 2000 *Phys. Rev.* B **62** 16356
Maier S A, Kik P G, Artwater H A, Meltzer S, Harel E, Koel B E and Requicha A A G 2003 *Nat. Mater.* **2** 229
[6] Valden M, Lai X and Goodman D W 1998 *Science* **281** 1647
[7] Schuck P J, Fromm D P, Sundaramurthy A, Kino G S and Moerner W E 2005 *Phys. Rev. Lett.* **94** 017402
[8] Ahmadi T S, Wang Z L, Green T C, Henglein A and El-Sayed M A 1996 *Science* **272** 1924
Daniel M C and Astruc D 2004 *Chem. Rev.* **104** 293
Schulz F, Franzka S and Schmid G 2002 *Adv. Funct. Mater.* **12** 532
Salata O V 2005 *Curr. Nanosci.* **1** 25
[9] Skrabalak S E, Au L, Li X and Xia Y 2007 *Nat. Protoc.* **2** 2182
Chen H, Kou X, Yang Z, Ni W and Wang J 2008 *Langmuir* **24** 5233
[10] Oldenburg S J, Averitt R D, Westcott S L and Halas N J 1998 *Chem. Phys. Lett.* **288** 243
[11] Kraus T, Malaquin L, Delamarche E, Schmid H, Spencer N D and Wolf H 2005 *Adv. Mater.* **17** 2438
[12] Xia Y N, Yin Y D, Lu Y and McLellan J 2003 *Adv. Funct. Mater.* **13** 907
[13] Kim Y H, Park J, Yoo P J and Hammond P T 2007 *Adv. Mater.* **19** 4426
[14] Maury P A, Reinhoudt D N and Huskens J 2008 *Curr. Opin. Colloid Interface Sci.* **13** 74
Huwiler C, Halter M, Rezwan K, Falconnet D, Textor M and Voros J 2005 *Nanotechnology* **16** 3045
Masuda Y, Itoh T and Koumoto K 2005 *Langmuir* **21** 4478
[15] Lopes W A and Jaeger H M 2001 *Nature* **414** 735
Morkved T L, Wiltzius P, Jaeger H M, Grier D G and Witten T A 1994 *Appl. Phys. Lett.* **64** 422
[16] Xu T, Kim H C, DeRouchey J, Seney C, Levesque C, Martin P, Stafford C M and Russel T P 2001 *Polymer* **42** 9091
[17] Black C T and Guarini K W 2004 *J. Polym. Sci.* A **42** 1970
[18] Segalman R A, Hexemer A and Kramer E J 2003 *Macromolecules* **36** 6831
[19] Sundrani D, Darling S B and Sibener S J 2004 *Nano Lett.* **4** 273
Edwards E W, Montague M F, Solak H H, Hawker C J and Nealey P F 2004 *Adv. Mater.* **16** 1315
[20] Stoykovich M P, Muller M, Kim S O, Solak H H, Edwards E W, de Pablo J J and Nealey P F 2005 *Science* **308** 1442
[21] Grabarek Z and Gergely J 1990 *Anal. Biochem.* **185** 131
[22] Turkevich J, Stevenson P C and Hillier J 1951 *Discuss. Faraday Soc.* **11** 55
[23] Mansky P, Liu Y, Huang E, Russel T P and Hawker C J 1997 *Science* **275** 1458
[24] Garcia R and San Paulo A 1999 *Phys. Rev.* B **60** 4961
Anczykowski B, Gotsmann B, Fuchs H, Cleveland J P and Elings V B 1999 *Appl. Surf. Sci.* **140** 376
[25] Peng J, Xuan Y, Wang H, Yang Y, Li B and Han Y 2004 *J. Chem. Phys.* **120** 11163
[26] Brown L, Koerner T, Horton J H and Oleschuk R D 2006 *Lab Chip* **6** 66
[27] Li Y, Pham J Q, Johnston K P and Green P F 2007 *Langmuir* **23** 9785
[28] Maury P, Escalante M, Reinhoudt D N and Huskens J 2005 *Adv. Mater.* **17** 2718
[29] Lee I, Zheng H, Rubner M F and Hammond P T 2002 *Adv. Mater.* **14** 572
[30] Zehner R W, Lopes W A, Morkved T L, Jaeger H and Sita L R 1998 *Langmuir* **14** 241